



# Deactivation of nickel-based anode in solid oxide fuel cells operated on carbon-containing fuels



Jie Xiao <sup>a</sup>, Yongmin Xie <sup>a</sup>, Jiang Liu <sup>a, b, \*</sup>, Meilin Liu <sup>b, c</sup>

<sup>a</sup> The Key Laboratory of Fuel Cell Technology of Guangdong Province, School of Chemistry and Chemical Engineering, South China University of Technology, Guangzhou 510641, PR China

<sup>b</sup> New Energy Research Institute, College of Environment and Energy, South China University of Technology, Guangzhou 510006, PR China

<sup>c</sup> School of Materials Science and Engineering, Georgia Institute of Technology, 771, Ferst Drive, Atlanta, GA 30332-0245, USA

## HIGHLIGHTS

- Carbon deposits on Ni–YSZ anode of SOFCs operated on CH<sub>4</sub> or CO.
- Deposition is limited by kinetics at low and thermodynamics at high temperature.
- Effects of C formation on anode correlates strongly between each other.
- High C solubility in Ni and strong C–Ni interaction cause the anode deactivation.
- Carbon formation on anode can be avoided by O<sup>2–</sup> flux through electrolyte of SOFC.

## ARTICLE INFO

### Article history:

Received 21 March 2014

Received in revised form

13 June 2014

Accepted 14 June 2014

Available online 21 June 2014

### Keywords:

Solid oxide fuel cells

Nickel-based anode

Carbon deposition

Carbon fiber growth

Deactivation mechanism

Carbon-containing fuel

## ABSTRACT

Deactivation of Ni–YSZ (yttrium stabilized zirconia) anode of SOFCs operated on CH<sub>4</sub> and CO, respectively, is investigated systematically. Experiments show that the rate of carbon deposition on Ni–YSZ substrate from CH<sub>4</sub> increases with temperature in the whole testing temperature range (550–800 °C), while the rate from CO increases with temperature at lower temperatures but decreases at higher temperatures. Larger amount of carbon deposit results in more significant substrate deformation and destruction, which can be explained by the mechanism of carbon fiber growth on Ni exposed to carbon-containing gases. Carbon deposition can be avoided by oxygen ion flux through the electrolyte of SOFCs operated on either CH<sub>4</sub> or CO.

© 2014 Elsevier B.V. All rights reserved.

## 1. Introduction

In the fuel cell family, the solid oxide fuel cell (SOFC), with all-solid-state structure, is standing out due to its high electrical conversion efficiency, easy maintenance, and practical fuel flexibility [1]. The SOFC can be developed into a low cost electricity generation technology because most readily available carbon-containing gases, such as hydrocarbons and monoxide, can be directly used as their fuels.

Ni–YSZ cermet is the most commonly used anode material of SOFCs, which shows good performance [2], because Ni has high electrical conductivity and relatively high electrocatalytic activity towards oxidation of H<sub>2</sub> and reforming of carbon-containing fuels. Meanwhile, YSZ distributed in the anode can effectively prevent Ni particles from coarsening under sintering and can broaden the triple phase boundary (TPB) for the anode reaction. However, the problem that Ni catalyzes carbon deposition reactions (1) and (2), resulting in deactivation of SOFC anode, has always been fatal for SOFCs operating on hydrocarbon or carbon-containing fuels.



\* Corresponding author. The Key Laboratory of Fuel Cell Technology of Guangdong Province, School of Chemistry and Chemical Engineering, South China University of Technology, Guangzhou 510641, PR China. Tel./fax: +86 02022236168.

E-mail address: [jiangliu@scut.edu.cn](mailto:jiangliu@scut.edu.cn) (J. Liu).

There have been numerous literature reporting on avoiding carbon depositions through improving the Ni-based anodes or developing alternative anode materials [3,4]. Based on thermodynamic calculations, partial oxidation and/or reforming of the fuels have been carried out by introducing  $O_2$ ,  $H_2O$ , and/or  $CO_2$  into the fuels to adjust the C:H:O ratio into the equilibrium range without carbon formation [5]. However, extra oxygen in the fuel results in lower voltage thus poorer performance. Therefore, anode catalysts that can promote electrochemical oxidation of carbon-containing fuels and inhibit carbon formation reactions have been developed. A simple example of the electrochemical oxidation catalyst is ceria. Steady operation of SOFCs with hydrocarbon fuels has been demonstrated by applying it as an interlayer between the YSZ electrolyte and Ni–YSZ anode [6] and as a component of Cu-based anode [7]. While many alternative anode materials can be operated on hydrocarbon fuels without carbon deposition, the performance of the corresponding SOFCs can not compare with that of the Ni-based anode SOFCs.

It is well known that Ni promotes carbon formation when exposed to carbon-containing gases [8] and the carbon forms may vary from high molecular weight hydrocarbons to primary carbons such as graphite, depending upon the conditions under which the deposit is formed and aged [9]. However, carbon deposition does not necessarily cause deactivation of a SOFC, because carbon itself can be used as fuel of SOFCs [10–12] and there is evidence that the deposited carbon can be directly oxidized by the oxygen ion coming through the electrolyte [13]. Moreover, there has been a report on hydrocarbon deposits enhancing the performance of a SOFC with Cu-based anode [14]. Nevertheless, in most cases, carbon formation on Ni-based anode causes serious deactivation of the anode and usually accompanied by mechanical cracking. To solve the problem of deactivation of Ni-based anode caused by carbon deposition, a clear knowledge on the conditions under which carbon deposition occurs and the mechanisms of the deactivation is necessary for applying proper method to improve the Ni-based anode for SOFCs operating on carbon-containing fuels with high performance.

Among the carbon-containing fuels,  $CH_4$  and CO are two of the most concerned.  $CH_4$  accounts for over 80% of natural gas which is a practical fuel for SOFCs [15]. CO is the main constituent of coal gas and is found in many biogases [16]. There have been many investigations on using  $CH_4$  or CO as the fuel of Ni–YSZ anode SOFCs. Serious carbon deposition of  $CH_4$  is always observed and this problem is commonly resolved through internal reforming by mixing large amount of steam with the fuel [17]. An alternative option is to flux oxygen ions to the anode by operating the SOFCs at a proper electrical current [15,18]. Being carbon-containing gas, CO is different from  $CH_4$  in the carbon deposition situation. While a SOFC stack has been reported to stably operate with dry CO for over 1000 h [19], more evidences have shown the negative effects of CO, appearing in fuels, on the performance of SOFCs with Ni-based anodes [20].

In the present work, carbon deposition of  $CH_4$  and CO on Ni–YSZ is systematically studied at SOFC operating conditions. The results are compared and analyzed based on thermodynamic equilibrium calculation, chemical kinetics and experimental measurements. The anode deactivation caused by carbon deposition is explained with the mechanism of the interactions between the Ni and a carbon-containing gas. The effects of oxygen ion flux, from the electrolyte of a SOFC operated at a proper current, on suppressing carbon deposition on the Ni–YSZ anode are investigated and analyzed.

## 2. Experimental

### 2.1. Fabrication of NiO–YSZ pellets and the whole cells

NiO (Australia) and YSZ (TZ-8Y, Building Material Academy of China) powders were mixed in a weight ratio of 1:1. In addition,

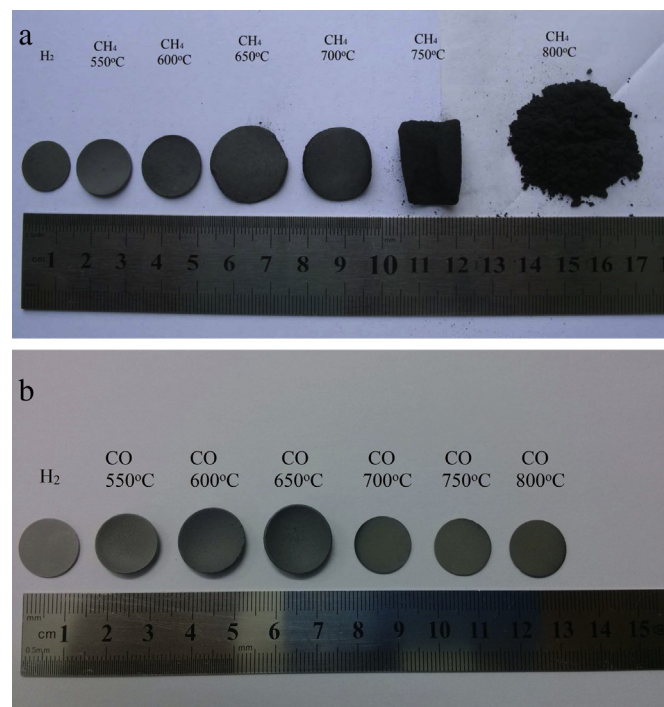


Fig. 1. Deformation of Ni–YSZ anode after respectively treated in  $CH_4$  (a) and CO (b) at different temperatures for 4 h.

10 wt.% starch was added as pore former to achieve sufficient porosity. Then the mixture was ground with a proper amount of ethanol in an agate mortar for 3 h and then thoroughly dried. Afterward the mixture powder was pressed into pellets of 15 mm in diameter and 0.6 mm in thickness under a pressure of 300 MPa [21]. The green pellets were sintered at 1400 °C for 4 h in air to get NiO–YSZ samples. To fabricate the button-type single cells, tape casting method was adopted to prepare the green NiO–YSZ anode supports, followed by pre-firing at 1100 °C for 2 h. Then, a thin layer of YSZ was coated on the pre-fired anode supports by dip coating method [22]. The green anode/electrolyte bi-layers were sintered at 1400 °C for 4 h to densify the YSZ film. At last, a layer of LSM (50 wt.%)–YSZ composite cathode and a layer of pure LSM cathode with an active area of 0.25 cm<sup>2</sup> were subsequently applied onto the

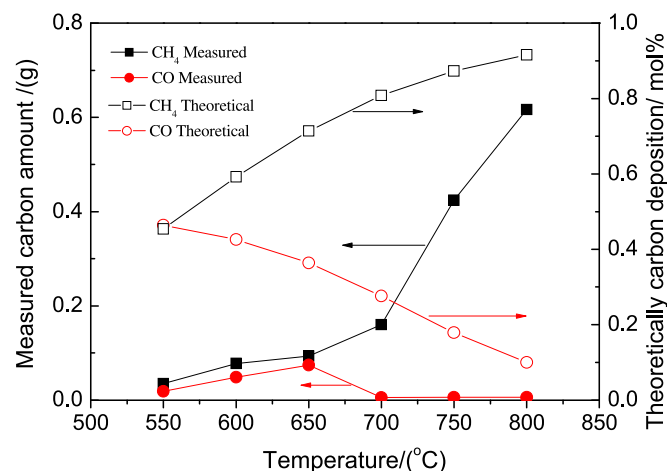


Fig. 2. Amount of carbon deposited on Ni–YSZ pellets after exposed to  $CH_4$  or CO for 4 h, at different temperatures.

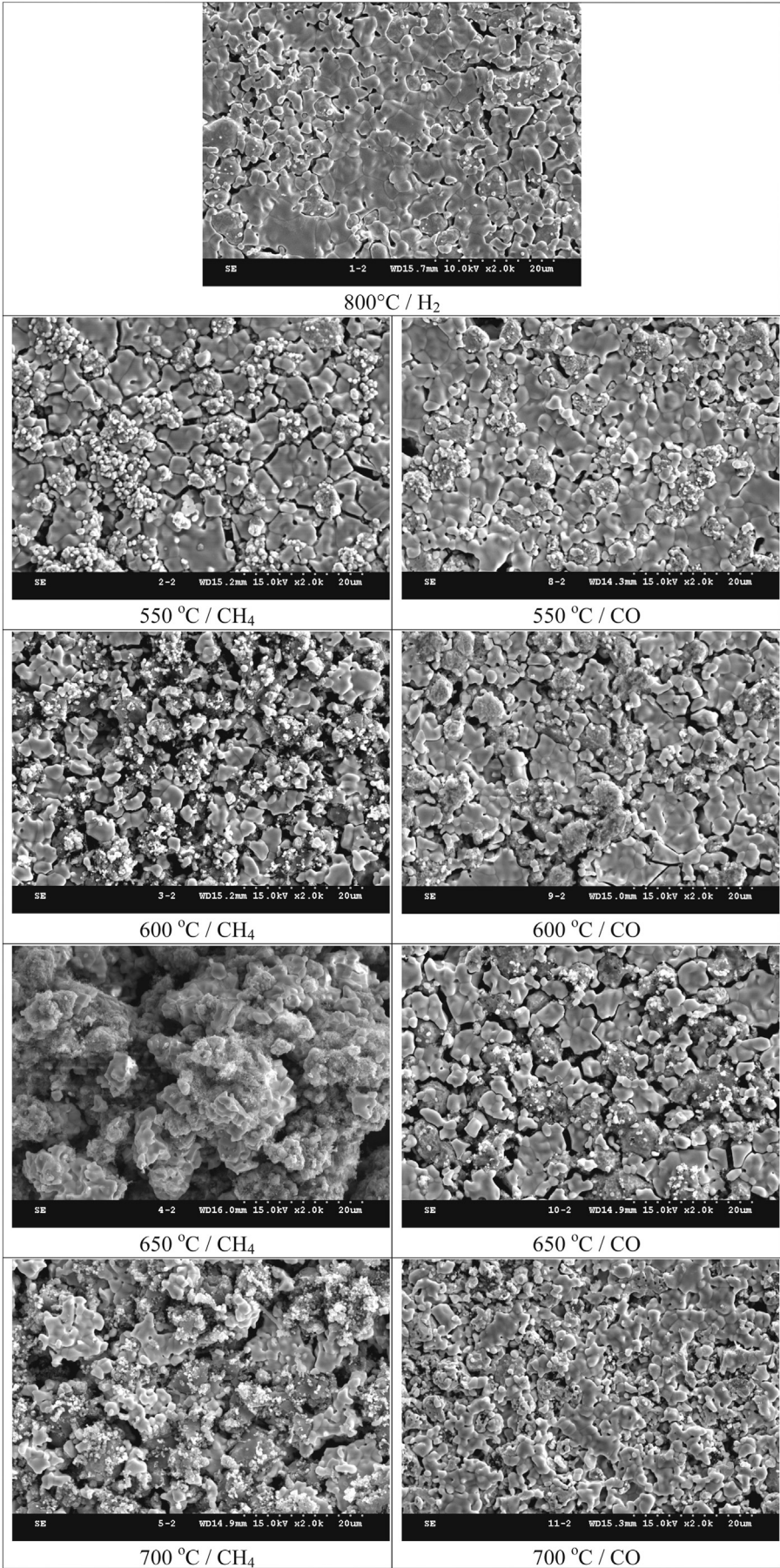


Fig. 3. SEM images of surfaces of Ni-YSZ pellets respectively treated in  $\text{CH}_4$  and  $\text{CO}$  at different temperatures.

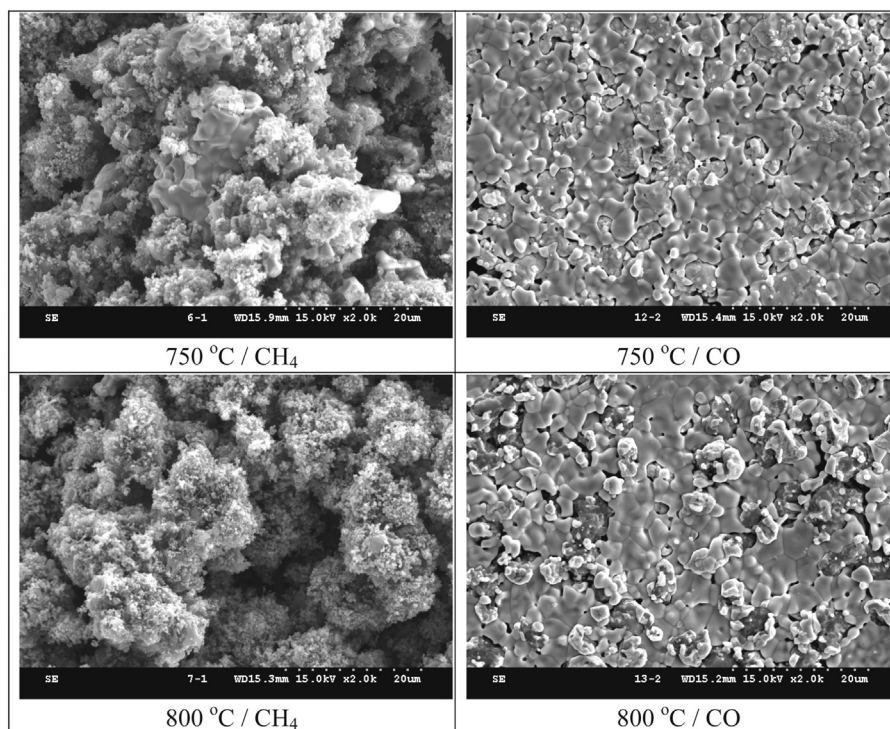


Fig. 3. (continued).

electrolyte surface by brush painting and fired at 1100 °C for 2 h. Silver paste (Shanghai Research Institute of Synthetic Resins, Shanghai, China) was used as current collector and sealant [23].

## 2.2. Carbon deposition on Ni–YSZ cermets exposed to carbon-containing gases

The NiO–YSZ pellets were placed in the middle of a long quartz tube with two ends sealed by rubber plugs and polytetrafluoroethylene sealing tape. The quartz tube was put into a tubular furnace, with the samples sitting at the middle (constant temperature zone). The set was heated while dry hydrogen was fed into the quartz tube at 800 °C for 1 h to completely reduce the NiO–YSZ to Ni–YSZ. Then, the set was cooled down to room temperature with hydrogen flowing. The Ni–YSZ pellets were removed and saved for the following tests. The weight of every Ni–YSZ pellet was about 0.37 g.

Each one of the Ni–YSZ pellets was used for testing at a certain condition. The pellet was placed in the middle of the long quartz tube and fixed by asbestos on both sides. The set, with hydrogen flowing through the tube, was heated to a certain temperature between 550 °C and 800 °C. Then the gas was switched to a dry carbon-containing gas (CH<sub>4</sub> or CO, 50 ml min<sup>−1</sup>) to make the Ni–YSZ pellet exposed to the fuel gas for 4 h. After that, the gas was switched to argon and the set was cooled down to room temperature under argon stream of 50 ml min<sup>−1</sup>. Finally, the pellet was weighed and the amount of carbon deposited was calculated.

## 2.3. Characterization

The electrochemical performance and stability test of the single cells were carried out by a four-probe set-up using Iviumstat electrochemical analyzer (Ivium Technologies B.V., Netherlands). Pure H<sub>2</sub>, CH<sub>4</sub> or CO at a flow rate of 50 ml min<sup>−1</sup> was respectively introduced to the anode while ambient air was applied as oxidant to the cathode.

The Ni–YSZ pellets after treatment and the cells after testing were characterized by scanning electron microscope (SEM, Hitachi S-4300) equipped with an energy dispersive X-ray spectroscopy (EDS). The thermodynamic equilibrium compositions calculations were carried out using a program, HSC chemistry (Version 6.0, Outokumpu Research Oy, Finland).

## 3. Results and discussion

### 3.1. Effect of carbon deposition on the deformation of Ni–YSZ anodes

Fig. 1 shows the deformation of Ni–YSZ pellets after respectively treated in CH<sub>4</sub> (a) and CO (b) at different temperatures for 4 h. The pellets reduced in H<sub>2</sub> are also provided as comparisons. It can be seen that the size of the pellets treated in CH<sub>4</sub> increases with treating temperature and the deformation is so serious at higher temperatures (700–800 °C) that the pellets are destructed. While in CO, the size of the pellets increases with temperature at lower temperatures (below 650 °C) but decreases at higher temperatures and remains almost unchanged above 700 °C.

Fig. 2 shows the carbon amount (g) deposited on the pellets after treated in CH<sub>4</sub> or CO for 4 h, at different temperatures. The theoretical predictions of carbon deposition based on thermodynamic equilibrium calculation are also provided as comparisons. As can be seen in Fig. 2, the experimental carbon deposition trend of CH<sub>4</sub> is basically in accordance with the thermodynamic equilibrium prediction, i.e., the amount of deposited carbon increases with temperature. However, the situation in CO is different. Although the thermodynamic calculation results show that carbon deposited from CO decreases with increasing temperature, the measured carbon increases with temperature in lower temperature range (<650 °C), which is similar to the situation of CH<sub>4</sub>. At higher temperatures, the carbon deposition decreases which seems consistent with the theoretical prediction.

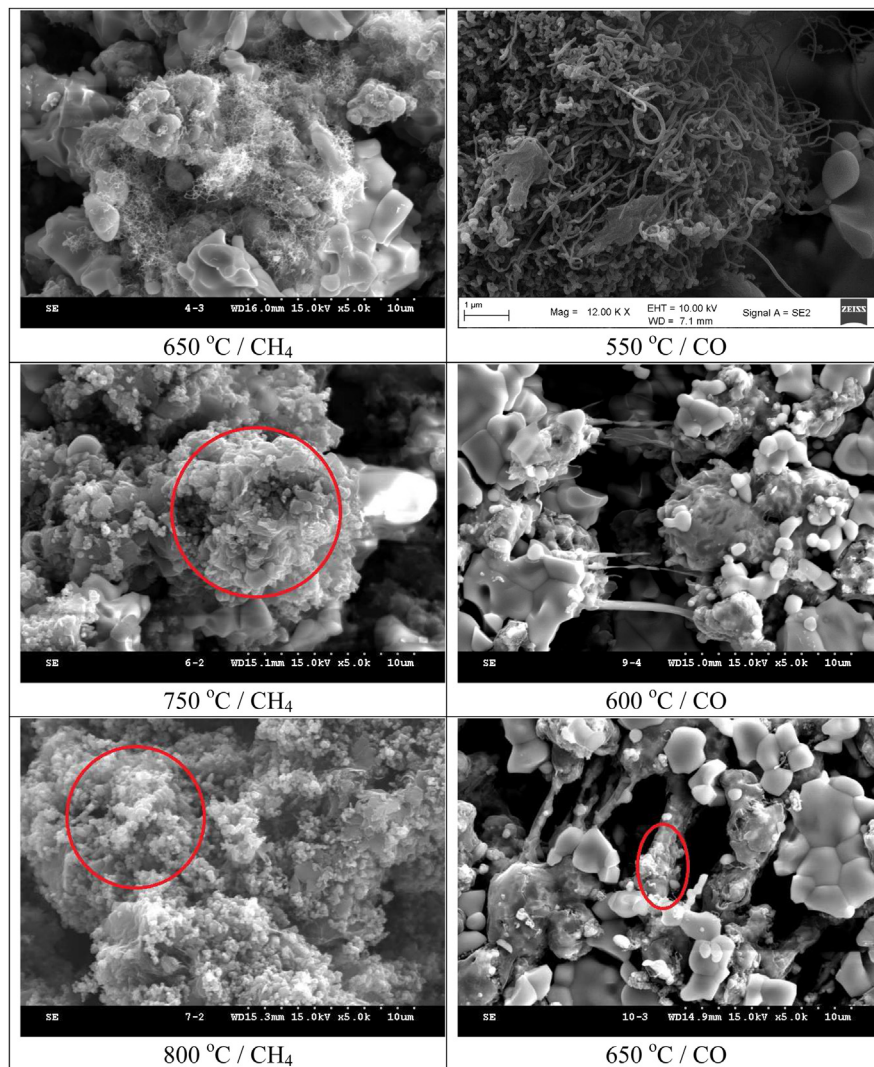


Fig. 4. SEM images of different forms of carbon deposition, with larger magnification.

According to chemical kinetics, the rate of a reaction is proportional to its rate constant  $k$ . For many reactions, the variation of rate constant with temperature can be expressed by the Arrhenius equation

$$\ln k = \ln A - \frac{E_a}{RT} \quad (3)$$

where  $A$  is the pre-exponential factor and  $E_a$  the activation energy. The experimental fact that carbon deposition of  $\text{CH}_4$  increases with temperature is understandable because thermodynamic equilibrium theory indicates that the right direction of reaction (1) is favored at high temperatures and chemical kinetics also suggests that its reaction rate increases with temperature. On the contrary, the reversed direction of reaction (2), according to thermodynamics, is favored as temperature increases, which is not supported by the experimental results of  $\text{CO}$  at lower temperatures, as shown in Fig. 2. This can be explained that, at low temperatures the reactant molecules can not get enough energy to overcome the activation energy so that the reaction rate is low, resulting in large deviation from the theoretical equilibrium. In other words, the reaction is controlled by chemical kinetics at lower temperatures. While at high temperatures, the reactions may approach equilibrium spontaneously and their extents are limited by thermodynamics.

The experimental results shown in Fig. 2 also correlate strongly with the deformation of the Ni–YSZ samples as shown in Fig. 1. Larger amount of carbon deposition (higher deposition rate) corresponds to more serious deformation. These evidences are related to the interactions between the carbon-containing gas and the Ni–YSZ samples, as will be explained later.

### 3.2. SEM analysis

Fig. 3 shows the surface SEM images of the Ni–YSZ pellets respectively treated in  $\text{CH}_4$  and  $\text{CO}$  at different temperatures. The image of the surface of a Ni–YSZ reduced in  $\text{H}_2$  at 800 °C is also shown as comparison. It is obvious that the change of surface morphology of the Ni–YSZ pellets has a strict corresponding relation to the deformation (Fig. 1) and deposited carbon amount (Fig. 2). Compared to the surface of the pellet reduced in  $\text{H}_2$ , the surface treated in  $\text{CO}$  at 750 °C and 800 °C, with neglected carbon deposit and shape deformation, is almost unchanged. Some cracks appear on the surface of those pellets treated in  $\text{CH}_4$  at 550 °C and 600 °C, in  $\text{CO}$  at 600 °C and 650 °C, all with light carbon deposition. Serious destruction occurs to the pellets treated in  $\text{CH}_4$  at high temperatures, with heavy carbon deposition.

It is well known that transition metals such as nickel, iron, and cobalt catalyze carbon formation from carbon-containing fuels, such as  $\text{CH}_4$ , CO and higher hydrocarbons. There has been a consensus that carbon deposition from the interaction between a transition metal and a carbon-containing gas involves three steps: First, carbon-containing molecules dissociate on the metal surface and carbon atoms are formed. Then, the carbon atoms dissolve in and diffuse through the bulk metal. Finally, the carbon atoms precipitate from the bulk on the other side of the metal [8]. Various carbon allotropes may be formed at different conditions. When there is a balance between the dissociation, diffusion, and segregation, carbon fibers will grow [24], as shown in the enlarged images of the carbon morphologies formed in  $\text{CH}_4$  at 650 °C or in CO at 550 °C, 600 °C and 650 °C, respectively (Fig. 4). At higher temperatures,  $\text{CH}_4$  becomes very reactive and the dissociation of  $\text{CH}_4$  molecules is so fast that the diffusion and segregation can not keep up with the carbon atom supply at the surface, resulting in encapsulating of Ni particles and no carbon fibers grow (Fig. 4). The carbon fiber growth and encapsulation on Ni–YSZ exposed to  $\text{CH}_4$  have also been observed and confirmed by Novosel et al. [25].

It has been extensively observed that nickel particles are lifted away from the bulk metal during carbon fiber growing, causing pulverizing of nickel metal. In this process, stress is arisen which results in destruction of the anode. For the situation at high temperatures, there is no carbon fiber growth, but the anode is destroyed more seriously. This might be explained from 3 aspects: (1) Encapsulating carbon, with a graphite structure, with large strength, deposited on the surface of Ni particles, may cause relatively large stress; (2) Ni particles are reshaped [26] during carbon fiber growth or carbon–Ni interaction; (3) Nickel is a face-centered cubic (FCC) crystal and carbon atoms may be dissolved in Ni bulk by occupying the interval sites of the FCC crystal cells, resulting in expansion of the bulk volume. The volume expansion causes severe inner stress of the anode, leading to damage of the pellet.

As a consequence, the cause of deactivation of Ni-based anode with carbon-containing fuels is the relatively strong carbon–nickel interaction and high solubility of C in Ni, which allows for carbon diffusion through the bulk of Ni. Those reported anode materials which can operate on hydrocarbon fuels with good stability, such as Cu and ceramics, are generally with little carbon solubility. These materials can not be destroyed by carbon deposition, even with large amount of carbon formation on the surface of the corresponding anodes [3,14,27,28]. Meanwhile, carbon is also formed by pyrolysis of methane at high temperatures. This form of carbon is different from that formed through diffusion and precipitation, it does not contribute to the destruction of the Ni-based anode [14].

### 3.3. Composition analysis on the Ni–YSZ surfaces

It is obvious that carbon deposited on the Ni–YSZ samples will change the surface composition. Although EDS analysis generally does not give accurate quantitative results, it can be applied to schematically present the relative fractions of elements C, Zr, and Ni on the treated Ni–YSZ surfaces, as shown in Fig. 5. Because the samples for EDS measurements are easily contaminated by the ambient  $\text{CO}_2$ , so there is a small fraction of C on the fresh Ni–YSZ anode surface and the amount of carbon is about 28 at.%. When treated in  $\text{CH}_4$ , the carbon deposition amount increases as the temperature rises. Meanwhile, when treated in CO, the carbon deposit first increases and then decreases with the temperature, consistent with the results in Fig. 2.

As the Ni–YSZ is made from NiO and YSZ with a weight ratio of 1:1, the atom ratio of Ni:Zr of the whole sample is about 2:1. However, the experimental Ni:Zr ratio at the surface is close to 1:1, which is reasonable because carbon deposits on Ni rather than on

Zr and more Ni surface is covered by carbon. Note that there is an abnormally high amount of Ni when treated in  $\text{CH}_4$  at 650 °C. This might be related to carbon fiber growth which is usually accompanied by a metal crystal at the top of the fiber [8].

### 3.4. The effects of oxygen ion flux on carbon deposition

Fig. 6 shows the performances of SOFCs with Ni–YSZ anode, respectively operated on (a)  $\text{CH}_4$  at 800 °C, (b) CO at 800 °C, (c)  $\text{CH}_4$  at 700 °C, and (d) CO at 650 °C. For each cell, the performance on  $\text{H}_2$  is better than that on  $\text{CH}_4$  or CO at the corresponding temperature, because of the higher mass of the carbon-containing fuel, which shows slower phase diffusion and lower electrochemical oxidation activity, resulting in polarization resistance increasing. Similarly, the cell yields poorer performance on CO than that on  $\text{CH}_4$  at 800 °C, as shown in Fig. 6(a) and (b).

Stability tests of the SOFCs with Ni–YSZ anodes operated on different conditions are shown in Fig. 7. Among the four selected temperature and fuel conditions, those corresponded by (a), (c), and (d) would cause serious damage of the anode if there were no electrical current through. However, Fig. 7 shows that when proper current is applied, the SOFCs with the Ni–YSZ anode can operate

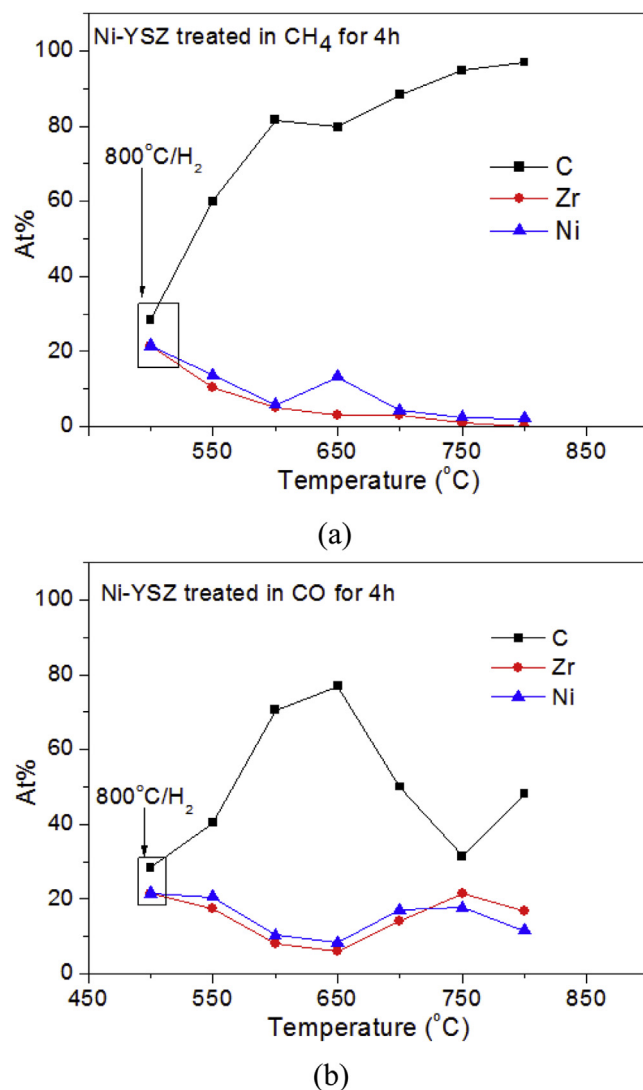


Fig. 5. Composition of the surfaces of Ni–YSZ anodes treated in different atmospheres at different temperatures: (a) in  $\text{CH}_4$  for 4 h; (b) in CO for 4 h.

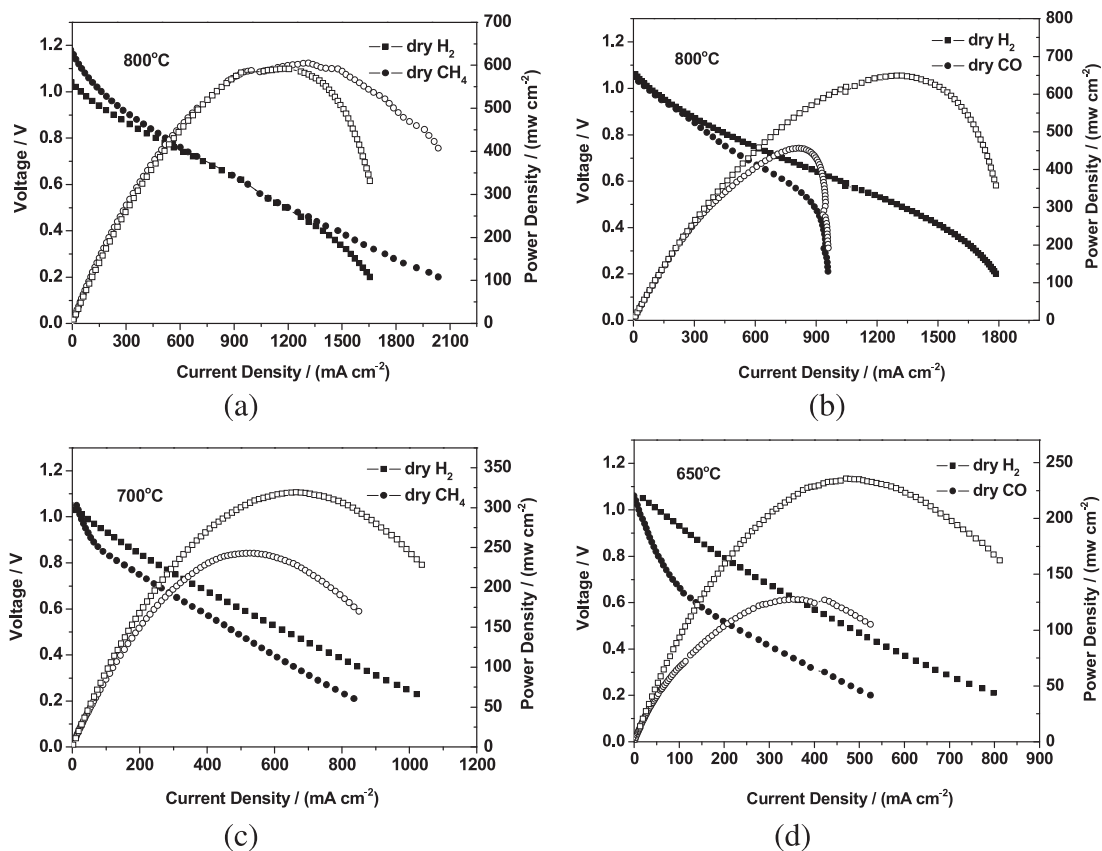


Fig. 6. Performances of SOFCs with Ni-YSZ anodes operated on (a) CH<sub>4</sub> at 800 °C; (b) CO at 800 °C; (c) CH<sub>4</sub> at 700 °C; and (d) CO at 650 °C.

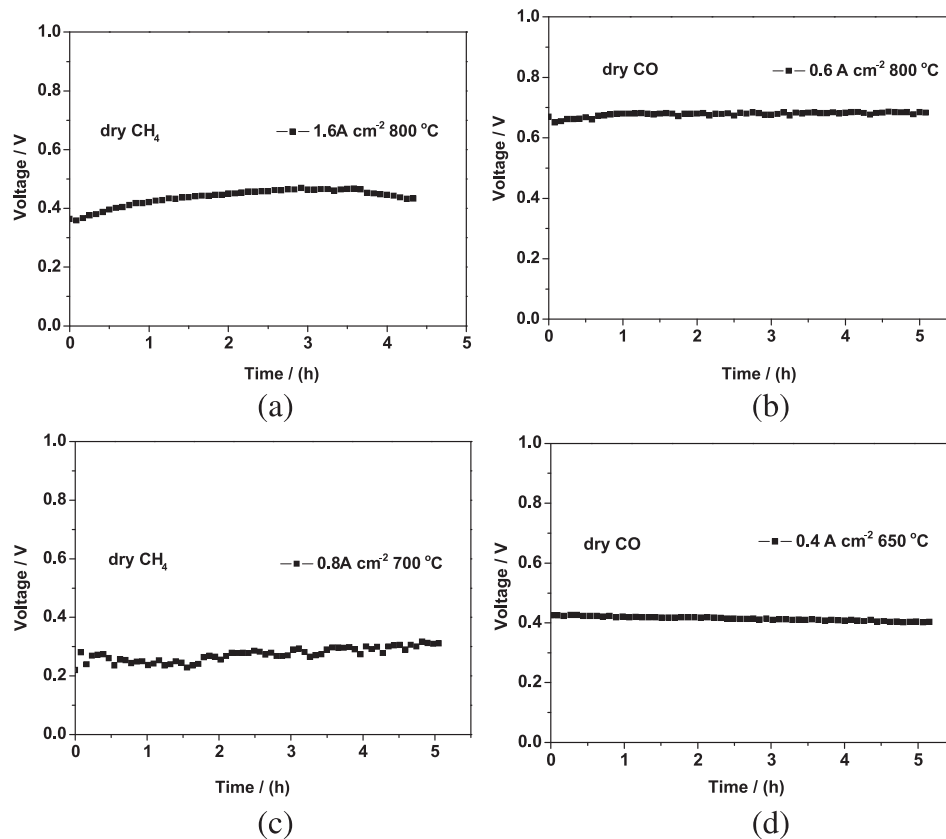


Fig. 7. Stability test of SOFCs with Ni-YSZ anodes operated on (a) CH<sub>4</sub> at 800 °C, with current density of 1.6 A cm<sup>-2</sup>; (b) CO at 800 °C, 0.6 A cm<sup>-2</sup>; (c) CH<sub>4</sub> at 700 °C, 0.8 A cm<sup>-2</sup>; and (d) CO at 650 °C, 0.4 A cm<sup>-2</sup>.

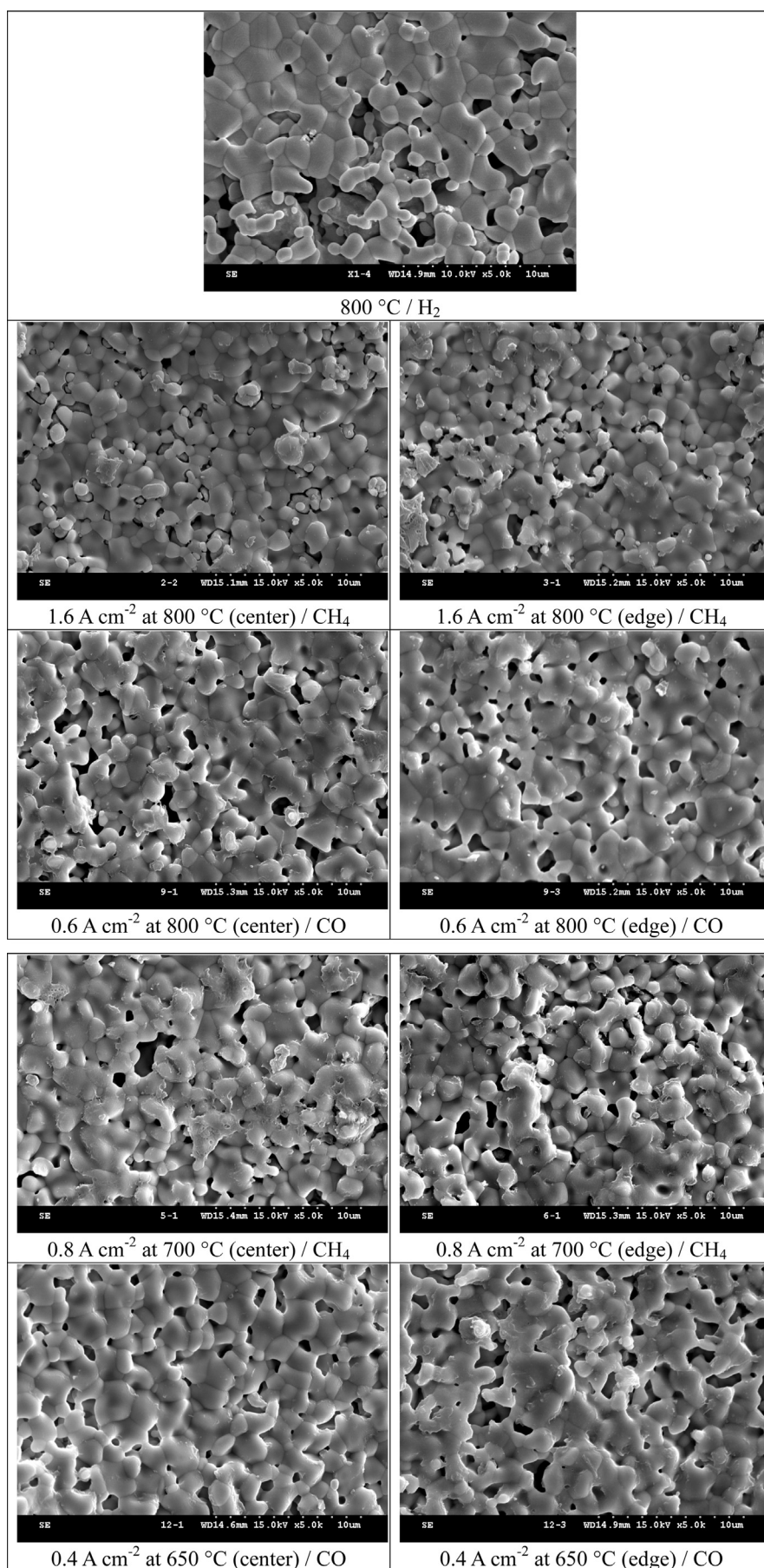


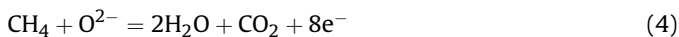
Fig. 8. SEM images of the Ni-YSZ anode surfaces of the SOFCs after stability testing.

under the four conditions with great stability (more than 4 h which has been the treatment time of the Ni–YSZ anode pellets under open circuit condition), demonstrating that oxygen ion flux through the electrolyte can eliminate the carbon deposition on Ni–YSZ anode from both CH<sub>4</sub> and CO [15].

There should be a lowest current density that can provide the minimum oxygen ion flux to remove the deposited carbon in time. However, the lowest current density varies with many details such as operating temperature, cell performance, fuel composition and flow rate, etc. Lin and Barnett et al. studied Ni–YSZ anode-supported SOFCs operated on humidified CH<sub>4</sub> (3% H<sub>2</sub>O) and they found that the cells were not stable at open circuit voltage at any operating temperature. While a current density of 0.1 A cm<sup>−2</sup> could maintain stable operation for the cells operated at 700 °C and below, much larger current, i.e., 0.8 A cm<sup>−2</sup> for 750 °C and 1.8 A cm<sup>−2</sup> for 800 °C, was necessary to keep the stability at higher temperatures [18]. In the present work, the value of current applied to each of the tested cell (shown in Fig. 7) is not necessarily the optimized or the lowest to maintain the operating stability. It is chosen based on a rough estimation that higher current should be applied to those cells which are more easily damaged or operate at higher temperatures.

Fig. 8 shows the SEM images of the Ni–YSZ anode surface morphologies of the SOFCs after stability testing. Also, the image of a fresh anode surface of Ni–YSZ is shown as comparison. Distinctly, it seems that the deposited carbon at the center part of the anode surface (so-called effective area which is counter to the cathode) should be removed more easily than the periphery/edge part. To compare these differences, the images of both the center part and the periphery part are shown. However, Fig. 8 shows there's no obvious difference between these two parts and the anode surfaces all keep integrated with no obvious carbon formation, which is in good agreement with the results of stability test results shown in Fig. 7.

There is a point of view that it is not possible to remove carbon from the SOFC anode by O<sup>2−</sup> flux through the electrolyte because O<sup>2−</sup> can only work within a limited region near the three-phase boundary, and, the elimination of carbon formation in a SOFC with high performance is due to generation of steam or CO<sub>2</sub> [29]. However, there is evidence showing that carbon deposited on the SOFC anode, in a pure argon atmosphere (without any steam or CO<sub>2</sub>), can be oxidized through current running (although after running some CO<sub>2</sub> is produced) [30]. According to thermodynamic equilibrium calculation, a steam to carbon ratio (molar ratio of H<sub>2</sub>O:CH<sub>4</sub>) or a CO<sub>2</sub> to carbon ratio (CO<sub>2</sub>:CH<sub>4</sub>) should be more than 1.2 or 2.4 to avoid carbon formation from methane at 700 °C [31]. Suppose that when a SOFC is operated with CH<sub>4</sub> under a current density of  $J$ , the cell reaction is



Then the production rate of CO<sub>2</sub> is

$$r_{\text{CO}_2} = \frac{60JSV_m}{8F} \quad (\text{ml min}^{-1}) \quad (5)$$

where  $S$  is the effective area,  $F$  the Faraday constant, and  $V_m$  the molar volume of ideal gas at standard condition. The consumption rate of CH<sub>4</sub> through the cell reaction is the same as  $r_{\text{CO}_2}$ , and the production rate of H<sub>2</sub>O is  $r_{\text{H}_2\text{O}} = 2r_{\text{CO}_2}$ .

For the present SOFC (with an effective area of 0.25 cm<sup>2</sup>) operated at 700 °C with CH<sub>4</sub> flowing at a rate of 50 ml min<sup>−1</sup>, at a current density of 0.8 A cm<sup>−2</sup> (Fig. 7c), it can be calculated that  $r_{\text{H}_2\text{O}} = 0.70 \text{ ml min}^{-1}$  and  $r_{\text{CO}_2} = 0.35 \text{ ml min}^{-1}$ . Thus the steam to carbon ratio and the CO<sub>2</sub> to carbon ratio are only 0.014 and 0.007, respectively, far below the equilibrium values for avoiding carbon formation. The carbon removal through O<sup>2−</sup> can not be simply

explained by a global thermodynamic equilibrium in the SOFC. Local equilibrium condition favored for carbon removal might be realized near the three-phase boundaries and direct oxidation of carbon might contribute to it. Even though, it is still hard to understand how the carbon at the edge part of the anode is avoided as the current density there is tens of times less than that at the center part. Much work is needed to reveal the mechanism of carbon formation or removal on a Ni-based anode with oxygen ion flux.

#### 4. Conclusions

A systematic investigation of carbon deposition on Ni–YSZ anode of SOFCs operated on CH<sub>4</sub> and CO shows that carbon deposits on Ni–YSZ at open circuit voltage (with no electrical current). At lower temperatures, the rate of deposition reaction is controlled by kinetics and at high temperatures it is limited by thermodynamics. There are strict correlations between each other of the carbon deposition rate, deformation of the sintered anode, and the microstructure morphology, i.e., larger amount a carbon causes more serious deformation and more disintegrated microstructure. The principle cause of deactivation or damage of Ni-based anode exposed to carbon-containing fuels is the high solubility of C in Ni and strong C–Ni interaction, which allow for carbon diffusing through the bulk Ni and depositing on Ni surface in the form of graphite. Carbon formation on the Ni–YSZ anode can be avoided by oxygen ion flux through the electrolyte but the detailed mechanism is still not clear.

#### Acknowledgments

This work was supported by the National Science Foundation of China (NSFC, Grant No. 21276097).

#### References

- [1] S.C. Singhal, *Solid State Ionics* 152–153 (2002) 405–410.
- [2] C.W. Sun, U. Stimming, *J. Power Sources* 171 (2007) 247–260.
- [3] A. Atkinson, S. Barnett, R.J. Gorte, J.T.S. Irvine, A.J. Mcevoy, M. Mogensen, S.C. Singhal, *J. Vohs, Nat. Mater.* 3 (2004) 17–27.
- [4] W. Wang, C. Su, Y. Wu, R. Ran, Z. Shao, *Chem. Rev.* 113 (2013) 8104–8151.
- [5] K. Sasaki, Y. Teraoka, *J. Electrochem. Soc.* 150 (2003) A878–A884.
- [6] E.P. Murray, T. Tsai, S.A. Barnett, *Nature* 400 (1999) 649–651.
- [7] S.D. Park, J.M. Vohs, R.J. Gorte, *Nature* 404 (2000) 265–267.
- [8] K.P. de Jong, J.W. Geus, *Catal. Rev. Sci. Eng.* 42 (2000) 481–510.
- [9] C.H. Bartholomew, *Appl. Catal. A Gen.* 212 (2001) 17–60.
- [10] Y.B. Tang, J. Liu, *Int. J. Hydrogen Energy* 35 (2010) 11188–11193.
- [11] Y.H. Bai, Y. Liu, Y.B. Tang, Y.M. Xie, J. Liu, *Int. J. Hydrogen Energy* 36 (2011) 9189–9194.
- [12] Y.M. Xie, Y.B. Tang, J. Liu, *J. Solid State Electrochem.* 17 (2013) 121–127.
- [13] C. Li, Y.X. Shi, N.S. Cai, *J. Power Sources* 196 (2011) 754–763.
- [14] S. McIntosh, J.M. Vohs, R.J. Gorte, *J. Electrochem. Soc.* 150 (2003) A470–A476.
- [15] J. Liu, S.A. Barnett, *Solid State Ionics* 158 (2003) 11–16.
- [16] T.M. Gür, M. Homel, A.V. Virkar, *J. Power Sources* 195 (2010) 1085–1090.
- [17] A.L. Lee, R.F. Zabransky, W.J. Huber, *Ind. Eng. Chem. Res.* 29 (1990) 766–773.
- [18] Y.B. Lin, Z.L. Zhan, J. Liu, S.A. Barnett, *Solid State Ionics* 176 (2005) 1827–1835.
- [19] M. Homel, T.M. Gür, J.H. Koh, A.V. Virkar, *J. Power Sources* 195 (2010) 6367–6372.
- [20] Y. Liu, Y. Bai, J. Liu, *J. Electrochem. Soc.* 160 (2013) F13–F17.
- [21] J. Ding, J. Liu, *Solid State Ionics* 179 (2008) 1246–1249.
- [22] Y.H. Zhang, J. Liu, J. Yin, W.S. Yuan, J. Sui, *Int. J. Appl. Ceram. Technol.* 5 (2008) 568–573.
- [23] J. Liu, W.H. Su, Z. Lv, Y. Ji, L. Pei, W. Liu, T.M. He, *Chinese Patent: CN02133049.2*.
- [24] M.L. Toebes, J.H. Bitter, A.J. van Dillen, K.P. de Jong, *Catal. Today* 76 (2002) 34–42.
- [25] B. Novosel, M. Marinsek, J. Macek, *J. Fuel Cell. Sci. Technol.* 9 (2012), 061003–1–7.
- [26] S. Helveg, C. Lopez-Cartes, J. Sehested, P.L. Hansen, B.S. Clausen, J.R. Rostrup-Nielsen, F. Abild-Pedersen, J.K. Nørskov, *Nature* 427 (2004) 426–429.
- [27] L. Yang, S.Z. Wang, K. Blinn, M.F. Liu, Z. Liu, Z. Cheng, M.L. Liu, *Science* 326 (2009) 126–129.
- [28] Y.H. Huang, R.I. Dass, Z.L. Xing, J.B. Goodenough, *Science* 312 (2006) 254–257.
- [29] S. McIntosh, R.J. Gorte, *Chem. Rev.* 104 (2004) 4845–4865.
- [30] M. Ihara, S. Hasegawa, *J. Electrochem. Soc.* 153 (2006) A1544–A1546.
- [31] K. Sasaki, Y. Teraoka, *J. Electrochem. Soc.* 150 (2003) A885–A888.